Internal Works Quality Assessment for Wall Evenness using Vision-based Sensor on a Mecanum-Wheeled Mobile Robot

Ahmad Zaki Shukor[1], Muhammad Herman bin Jamaluddin[2]
Mohd Zulkifli bin Ramli[3], Ghazali bin Omar[4], Syed Hazni Abd Ghani[5]
Faculty of Electrical Engineering, Universiti Teknikal Malaysia Melaka, Malaysia[1, 2, 3]
Advanced Manufacturing Centre, Universiti Teknikal Malaysia Melaka, Malaysia[4]
Construction Quality Assesment Centre (CASC), Construction Research Institute of Malaysia (CREAM), Malaysia[5]

***Abstract*—Robotics in the construction industry has been used for a few decades up to this present time. There are various advanced robotics mechanisms or technologies developed for specific construction task to assist construction. However, not many researches have been found on the quality assessment of the finished structures. This research proposes a quality assessment robot that will assist in performing the assessment of the internal works of a building by assessing a quality assessment criterion in the Malaysian Construction Industry Standards. There are various assessment criteria such as hollowness, cracks and damages, finishing and jointing. This paper will focus on the wall evenness using a camera mounted on a mobile robot with a Mecanum wheel design. The wall evenness assessment was done via projecting a laser leveler on the wall and capturing the images by using a camera, which is later processed by a central controller. Results show that the deviation calculation method can be used to differentiate between even and uneven walls. Pixel deviations for even walls show values of less than 15 while uneven walls show values of more than 20 pixels.**

***Keywords*—Construction industry standards; internal works quality assessment; vision; Mecanum wheels**

I. Introduction

In this era of Industrial Revolution 4.0, many technologies are being used in various application areas. Internet-of-Things, virtual reality, data analytics, additive manufacturing and robotics are some of the interesting technologies that have accelerated various manufacturing sectors throughout the current years. In the construction industry, robotics has been applied since the early 1980's. In the Japan visit, Dr. James S. Albus from National Bureau of Standards [1] and six construction companies (Taisei Corporation, Takenaka, Hazama Gumi Ltd, Shimizu Construction, Kumagai Gumi Company and Toshiba Nuclear Group) had large research on budgets for construction robotics. There are many related researches of cooperative or multi-robots that were proposed in construction environment, such as multi-robot teleoperation using humanoid and legged robots [2], multi-robot material deposition using autonomous mobile robot extruder platform [3], human-robot collaboration for interior finishing [4] and distributed climbing strut robots that was used for guiding construction [5]. There were also studies on simulating robots in construction via haptic control for drywall installation, painting, welding, bolting and concrete pouring [6]. In another research, a robot was proposed for monitoring the work progress in a building construction site [7] and a façade cleaning robot was proposed in [8].

However, not many researches have been focused on the automated internal or external works of finished building or construction sites. At present, the quality assessment is performed by manual inspection by a human assessor or a panel of assessors. This is tedious and tiring work because assessors usually complete a substantial amount of sample houses or buildings within a few days. The research of a custom-built quality assessment robot could reduce the burden of human inspectors by carrying out assessment of some criteria of the structure quality. A bridge statics assessment robot for flood evacuation planning was designed by Maik Benndorf et al. in [9]. This is an example of an external structure assessment that uses vibration measurement sensors mounted on an Unmanned Ground Vehicle equipped with a robotic manipulator. For internal works, a custom-designed quality assessment robot was proposed by Rui-Jun Yan et al. [10]. In assessing the different criteria, Rui-Jun Yan attached several devices for the quality assessment robot, Quicabot. A thermal camera was used to assess the hollowness of the ground and walls, an RGB camera to detect cracks on the ground and walls, a laser scanner to measure the evenness of the ground and walls and alignment of two connected walls while an inclinometer to measure the inclination of the ground.

The use of laser projection and vision sensors were seen in other applications. Andrzej Sioma used laser and a camera to measure the surface defect of a ceramic tile [11]. The longitudinal rip of conveyor belt detection was performed by Xianguo Li et al. using laser-based machine vision in [12] because of the use of such belt mechanisms to transfer materials or products. Other than that, bubble defects on tire surface were also detected by Hualin Yang et al. in [13] by using laser and machine vision. Daniel Lopez-Escogido et al. [14], detected small defects in PCB using 2-D high precision laser sensors, which investigated high errors of units of micrometers due to the small outline of Surface-Mount-Devices (SMD).

Jorge Rodríguez-Araújo and Antón García-Díaz [15] investigated in-line Defect Classification and localization in Solar Cells for Laser-Based Repair. This is because the faulty

cells need to be identified to be repaired. In [16], Dong-Gi Woo et al. used multi-lasers to perform the inspection of the surface of a car door chassis by using a robot arm manipulator projecting the lasers in different poses, which could be used as a 3D measurement system. Other than that, Ting Lei et al. [17] used laser vision to identify thermal deformation of tube sheet welding by using a Cartesian robot, CCD camera, hoop assembly, laser sensors and single-line lasers. A combination of line scan camera and frame camera was used to detect product surface defects by applying the ideas of both surface grayscale image and depth image simultaneously [18] in which Zhen Liu et al. claim the accuracy of 0.13mm within a measurement of 500x300x200 mm^3. In [19] Simone Pasineet et al. investigated in-line monitoring of laser welding using vision system, which applied thresholding, binarization and blob-counting to robustly detect joint and obtain optimal acquisition of the melt pool during welding.

The weld seam detection and feature extraction of butt-welding was investigated by Wang Xiuping et al. [20] in which the laser stripe edges were detected. The welding was performed by a welding robot arm manipulator. Feature extraction of butt-joint was also investigated by Yuanyuan Zou et al. [21] which used three-line stripe laser vision sensor. The algorithm uses Laws texture energy filter, Canny operator, thresholding and textural feature; laser stripes were used as its feature points.

Although there is not much research or references in the area of building quality assessment using robots, the idea of using laser projection and image acquisition and processing has been used in some applications mentioned previously, i.e. weld seam identification, and defect detection of tiles or panels.

For this paper, our objective is to explore and propose quality assessment of a criterion in the Construction Industry Standards for internal works, which is the wall evenness assessment. We propose the use of laser projection and image processing for the assessment. A custom-made mobile robot was designed and developed for the assessment, which can be further upgraded to include assessment of other criteria such as hollowness, cracks and damages, wall alignment and others. The advantage of our method is the use of cost-effective devices such as laser leveler and standard High Definition (HD) USB cameras.

II. The Construction Quality Assessment Robot

The robot for the quality assessment of internal works was custom-built as shown in Fig. 1. Fig. 1(a) shows the 3D drawing of the robot and Fig. 1(b) shows the actual robot. It is a mobile robot equipped with the sensors used for assessment. The base of the robot which is mostly rectangular is driven by four planetary geared motors connected to couplings of the Mecanum wheels to enable multi-direction motion of the mobile robot. The details of the components are shown in Table I.

As described in Table I, there are several parts that are required for the robot to function. It includes the robot base, power supply, controllers, sensors and tapping rod mechanism. The robot structure is custom-built using the frames consisting of 20 x 20 aluminum profiles with a square base of 300 x 300 mm^2 size.

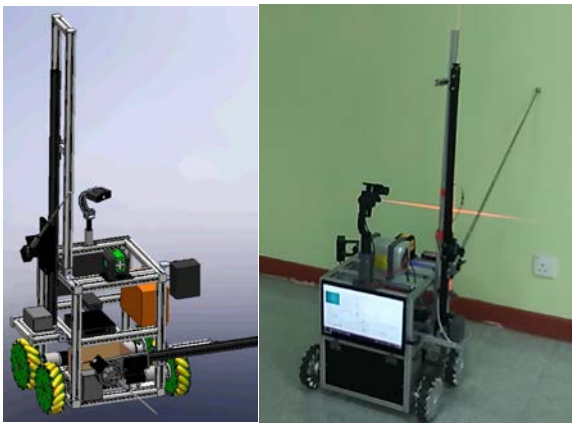

(a) (b)

Fig. 1. 3D Drawing of the Assessment Robot, (b) Actual Robot.

TABLE I. Quality Assessment Robot Components

Main Part	Sub-component	Details
Robot base	Planetary-geared DC motors (4)	24V 148RPM 18kgfcm 45mm
	Coupling (4)	10mm Key Hub for 152mm Mecanum Wheel
	Mecanum wheel (4)	152mm
	Structure	Aluminum Profile 2020, 300mm length each
	Motor Drivers (2)	10Amp 5V-30V DC Motor Driver (2 Channels)
Power supply	36 V DC Batteries	Rechargeable Lithium Ion 36V Batteries with BMS
	DC-DC converters	24V, 9V
Controller	Mobile Robot Controller	Arduino Pro-Mega
	Data acquisition and Processing	Intel BOXNUC8i6BEH3 (Intel i5)
	Display	13.3 inch USB-C Monitor
Sensors	Ranging sensors (8)	Time of Flight (TOF) VL 53L0X
	Corner alignment sensor	Time of Flight (TOF) VL 53L0X
	Camera (4)	2MP Webcam
	Laser leveler Gimbal	1-axis, mounted with camera
Tapping Rod	Slider	V-Slot Y-axis slider with Belt Buckle
	Servo Motor	4.5 – 6.0V RC Servo Motor
	Aluminum	V-Slot Aluminum Profile (Black Anodized) 2020
	Tensioner	Timing Belt Tensioner 2020

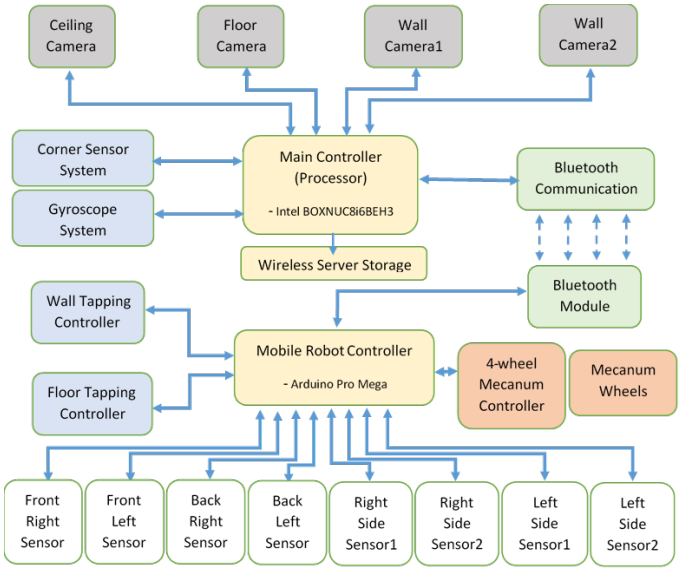

Fig. 2. Overall Block Diagram of the Quality Assessment Mobile Robot.

The overall block diagram of the Quality Assessment Robot is shown in Fig. 2. It consists of two main parts/controllers, which are the Main Processor and the Mobile Robot Controller. The main controller parts consist of the Central Processing Unit (CPU), four High Definition (HD) cameras, the corner sensor system and the gyroscope sensor system. The Mobile Robot Controller controls the four motors which are connected to the Mecanum wheels, the two tapping rod mechanisms which actuate the tapping rod motion and the interface with the eight (8) proximity sensors (Time-Of-Flight sensors).

The reason for using four cameras simultaneously is to enable four snapshots that can be taken which cover two walls (lower and upper), floor and ceiling view. This method can save time because it captures images at the same time, rather than moving a camera in different angles to capture the four images. The mechanical motion is only for the navigation of the mobile robot base. For the purpose of quality assessment, the obstacle detected using the proximity sensors is the wall it faces. Two sensors are placed at each side of the robot for the robot to navigate around its surroundings. The front side has two sensors to sense the wall facing the robot, the right side has two sensors to sense the right wall, the left side has two sensors to sense the left wall and the rear side has two sensors to sense the wall facing the robot's rear.

The mobile robot controller actuates the tapping rod movement, which is the wall tapping rod mechanism and the floor tapping rod mechanism. The wall tapping rod mechanism is located at the right side of the robot while the floor tapping rod mechanism is placed at the front side of the robot, as shown in Fig. 3. This tapping mechanism which consists of a tapping rod, a microphone and sliding mechanism, is used to assess the hollowness of the wall and floor by acquiring the sound waves recorded by the microphone attached to the tapping mechanism. However the tapping mechanism is not the focus in this paper.

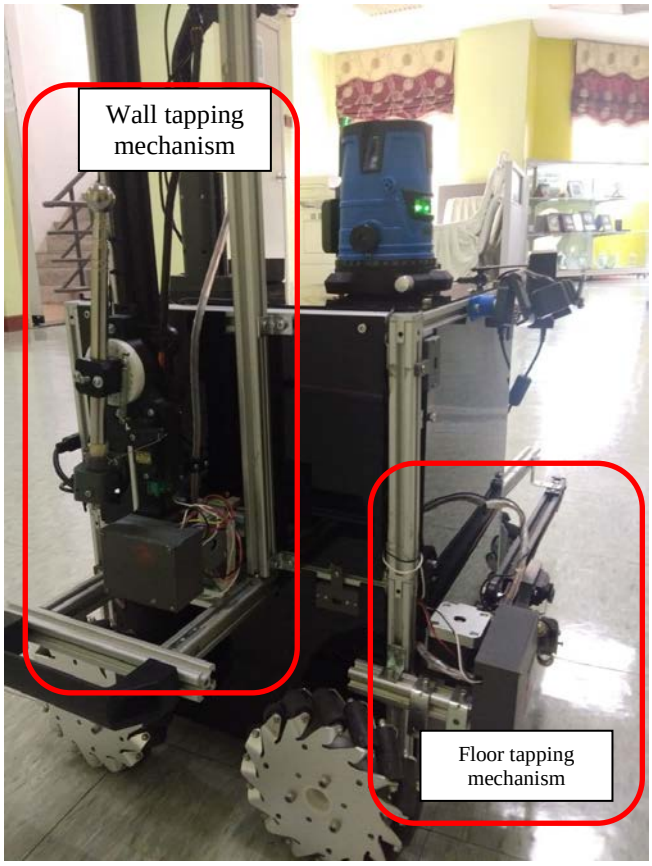

Fig. 3. The Wall-tapping Mechanism and Floor-tapping Mechanism.

The main processor controls the overall data acquisition of the mobile robot, such as image acquisition and processing, corner sensor data acquisition and evenness data acquisition. The pictures of the main processor-connected components are shown in Fig. 4.

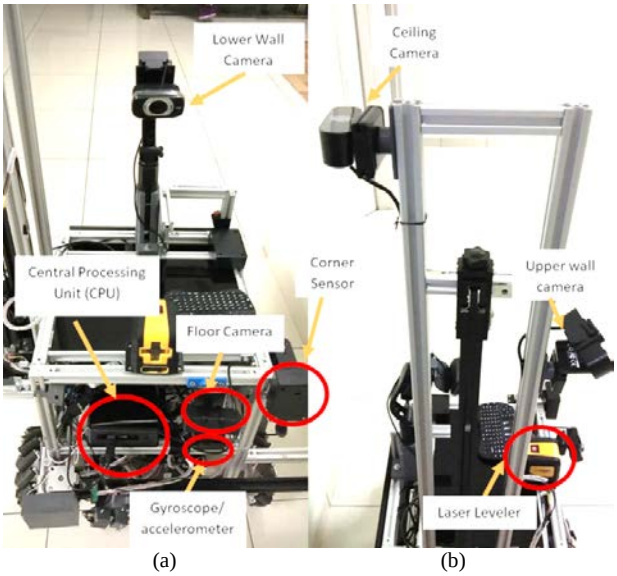

(a) (b)

Fig. 4. (a) The Floor Camera and Lower Wall Camera Connected to the CPU, (b) The Laser Leveler, Upper Wall Camera and Ceiling Camera.

The four cameras consist of a camera for the floor image capture, a camera for the ceiling image capture, a lower wall camera for capturing the image with the laser leveler projected lines and an upper wall camera to capture the upper wall area. These cameras are connected to the CPU and controlled by a custom-developed software. The laser leveler is attached on the upper frame of the robot, at a suitable height for the lower wall camera to capture the image. The other two cameras are located on the tapping rod holding frame, which is the upper wall camera and the ceiling camera.

There are two external sensor systems connected to the CPU; the corner detection sensor system and the gyroscope/accelerometer sensor system. These two sensors will record data and send it to the CPU for storage and processing. The data collected by the CPU (images, accelerometer readings, corner sensor readings) are stored in the wireless server data storage provided. The wireless server is accessed via the Wi-Fi network established between the CPU and the server. For the robot to move, the main controller will send commands to the mobile robot controller, which is connected to the CPU using Bluetooth Serial Port connection.

The simultaneous multi-assessment capability of the mobile robot is the clear advantage, acquiring different data for different criteria in the Quality Assessment System in Construction (QLASSIC) Construction Industry Standards. Its purpose at this time is not to replace the human assessor completely, but to assess some criteria. Hence it will lessen the burden of the human assessor and save time to complete a full assessment.

III. The Wall Evenness Assessment using Vision-based Approach

For this paper, we will focus on the wall evenness assessment using vision-based approach. The intention of applying the mobile robot into the construction assessment is to assist in assessing compliance with the Malaysian Construction Industry Standards (CIS). In the Standards, the wall surface evenness is considered “comply” if the deviation of wall surface is within 3mm, measured by 1.2m spirit level and steel wedge held by a human assessor. When the spirit level is placed on the wall, the steel wedge will be inserted in areas where there is space between the spirit level and the wall. This space should be within 3mm. This method using human assessment will depend on the consistency of human assessor evaluation. While some assessors take large samples of the wall in a room, others may only take samples of wall that he/she sees as a probable defect. This is due to the large number of rooms that the assessor is assigned to evaluate. This inconsistency is due to the human factor.

Thus, to assist the assessment, the mobile robot will help in acquiring images and later processing the images to determine wall evenness. By using a mobile robot, the image acquired will be at consistent distances set in the mobile robot controller program. The arrangement or setup of the mobile robot to acquire the images is illustrated as shown in Fig. 5.

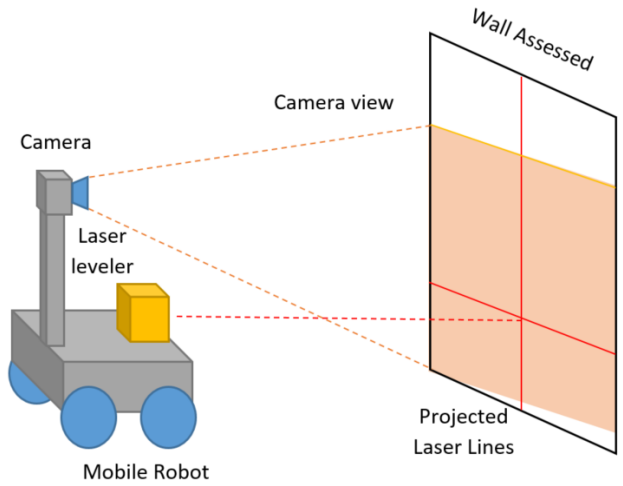

Fig. 5. Illustration of Image Capture of Wall for Surface Evenness Assessment.

The idea is to project the laser lines from the laser leveler to the wall facing the robot. At the same time, the camera mounted on the mobile robot will be able to view the laser lines on the surface of the wall. Then the image will be captured by the camera that contains the picture of the wall with the projected laser lines. The lines will not be deflected/deviated if the surface of the wall is even. If the lines are broken or deviated, it is an indication of non-compliance to the surface wall evenness criteria.

When measuring the wall, the robot navigates around by using the proximity sensors to slide left to be while maintaining its front to be parallel with the wall. This sliding motion is only possible by using the Mecanum wheels arrangement using the four DC motors driving the wheels. The sliding motion is shown in Fig. 6 and the motion of the robot inside a rectangular-shaped room is shown in Fig. 7. The robot in Fig. 7 is facing the wall on the right side. In short, the robot will automatically navigate around a rectangular-shaped room and stop evaluation once it reaches the fourth corner (start position).

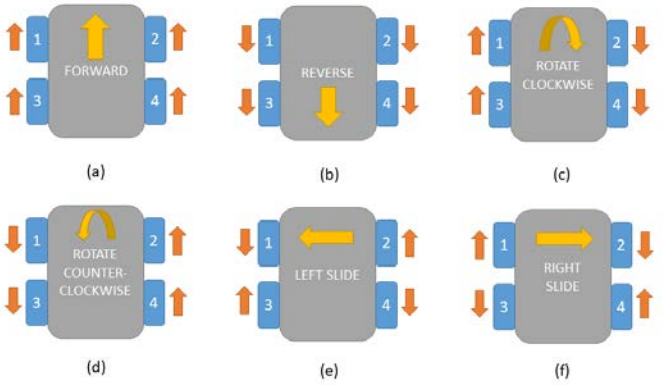

Fig. 6. Illustration of Mecanum Wheel Motions.

The Mecanum wheel motions (top view) in Fig. 6 shows the six different motions used for the mobile robot. The wheels are labeled as 1, 2, 3 and 4. With the right combination, different motions can be realized. The basic motions labeled as (a), (b), (c) and (d) shows the forward, reverse, rotate clockwise and rotate counter-clockwise motions of the mobile robot base. The other two motions, (e) and (f) are the sliding motions, in which (e) is left-slide motion while (f) is right-slide motion. Although the Mecanum wheels allow a lot more motions such as diagonal motions, the six motions in Fig. 6 is sufficient for the quality assessment mobile robot.

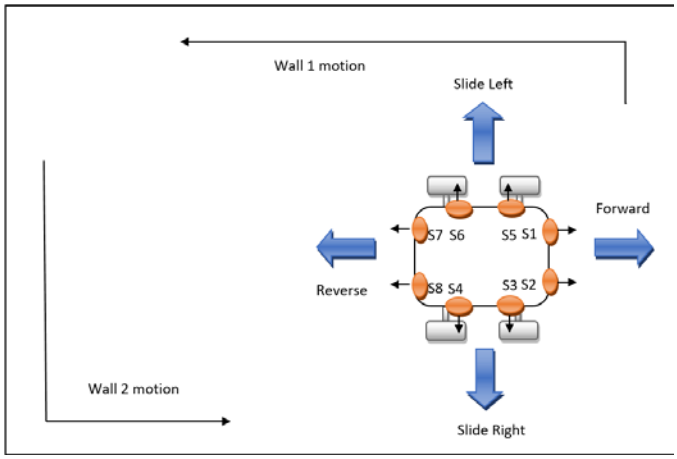

Fig. 7. Illustration of Sliding Motion during Wall Assessment.

The motion of the robot in the rectangular shaped room in Fig. 7, is performed by using the proximity sensors, for example, for the sliding left motion, sensors S1 and S2 will be used to follow the wall, while sensors S5 and S6 will be used to detect the first corner (top right in Fig. 7). After arriving at the corner, the robot will rotate itself counter-clockwise until it sensors the wall by using sensors S1 and S2. After that, it will perform the sliding left motion until it reaches the wall corner, completing the Wall 1 motion in Fig. 7. Similarly, Wall 2 motion will be performed after Wall 1 motion. During the sliding motion, the robot will stop momentarily, to acquire the images of the wall to be processed later. This is because if the robot acquires images while moving, the image might be blurred and causes difficulty for image processing. For a wall motion, there could be several images acquired, depending on the length of the wall. The distance between the robot and the wall is set at 60cm. If the distance is too short, the images captured will not cover enough area of the lower wall.

The image processing that needs to be done on the captured camera image, is HSL color filtering, Grayscale Conversion, Thresholding. By defining the range of acceptable color for the Red Laser line using HSL, the processing of the image will produce a black and white image. The white connected dots in the image will show the laser lines while the other colors will be turned to black.

Next, further image processing can be done, such as convex hull identification from blob, which will produce coordinates of the edges of the hull covering the vertical and horizontal laser line. The next step is to draw a red line from the top edge to the bottom edge to compare with the white lines of the laser leveler. The details of all these processes will be explained and shown in Section IV.

IV. Results and Analysis

For the site-testing of the mobile robot, the images are acquired from a finished housing area in Pulau Sebang, Melaka in September 2021. Additionally, the Skyworld Quality Center was also visited for another site-test for the mobile robot, in October 2021. The process for the image processing on the acquired images is shown in Fig. 8.

The results of image acquisition and processing are shown in Fig. 9.

The image in Fig. 9(a) shows a clear red-line projected image captured by the camera on a white-colored wall surface at the first site test, a house in a residential area in Pulau Sebang. The images acquired from the second site test at Skyworld Quality Centre are shown next in Fig. 9(d). This time the color of the wall is not white, but light yellow and the wall is uneven. Nevertheless, the red lines are still seen in the images. The sample image in Fig. 9(d) shows a slightly deflected vertical line.

The images in Fig. 9(a) are then color-filtered using Hue, Saturation, and Luminance (HSL) filtering from AForge library in Visual Studio (C #Net). The values used for HSL is 320 – 50 for Hue, 40%-100% for saturation and 40%-100% for luminance. These values are suitable for the red lines from the laser leveler. The results of the HSL filtering are shown in Fig. 9(b). For the image in Fig. 9(d), the same process is applied and the result image is shown in Fig. 9(e).

It can be seen in Fig. 9(b) and Fig. 9(e), the red lines were successfully seen and other backgrounds were eliminated. The next process is the Grayscale filtering and the Thresholding to ensure the image consists of only black and white colors for the next process to take place. For grayscale filter, the parameters are the values suggested from the AForge Grayscale filter library (0.2125, 0.7154, 0.0721). Grayscale filtering results are shown in Fig. 9(c) and Fig. 9(f).

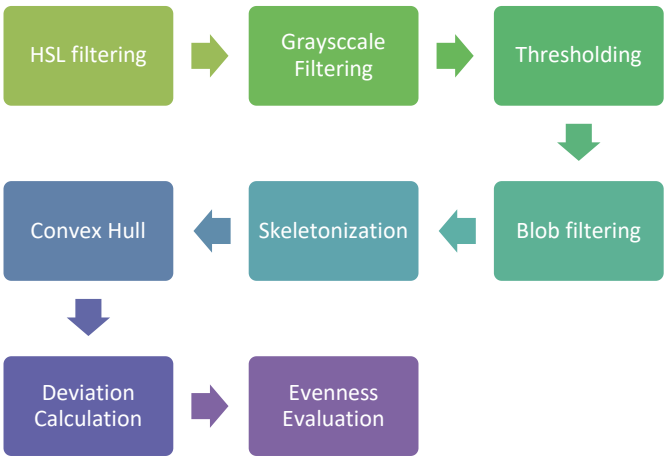

Fig. 8. Image Processing Method for the Wall Evenness Quality Assessment.

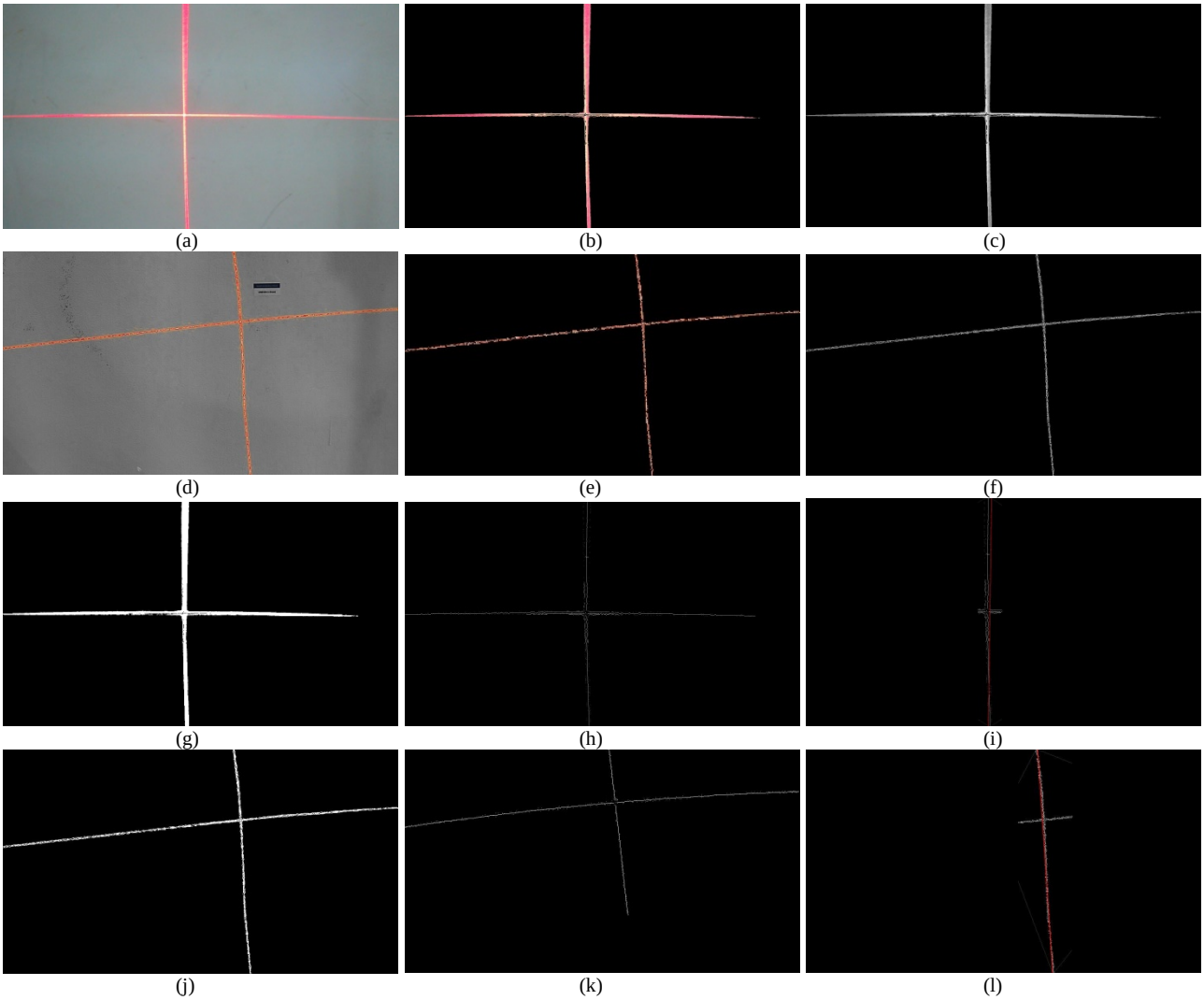

Fig. 9. Image Processing Results; (a) Image Acquired for Even Wall, (b) HSL Filtering on Even Wall, (c) Grayscale Filtering on Even Wall, (d) Image Acquired for Uneven Wall, (e) HSL Filtering on Uneven Wall, (f) Grayscale Filtering on Uneven Wall, (g)Thresholding Result on Even Wall, (h) Convex Hull of Even Wall, (i) Connected Edge Lines for Pixel Deviation of Even Wall, (j)Thresholding Result on Uneven Wall, (k) Convex Hull of Uneven Wall, (l) Connected Edge Lines for Pixel Deviation of Uneven Wall.

The next process after grayscale filtering is thresholding. For thresholding, the value set to allow the line to be converted to white color is 80. Values of grayscale below 80 will be turned to black color. This is to ensure that the Blob filtering process can take place, as it only receives black and white images. Thresholding results are shown in Fig. 9(g) and Fig. 9(j).

After thresholding, blob filtering is then applied, and then skeletonization. This is because blob filtering will extract blob sizes which are more than a certain width and height, in this case it is set at a width of 70 and height of 70. Any blobs smaller than this size will be neglected because it may consist of small errors which are not from the red line processed. Skeletonization is later applied to ensure that the line is thin for the next process.

Once skeletonization has been completed, the convex hull determination is performed to detect the top, bottom, most-left and most-right points that cover the blob. This is to ensure that the lines are all in one blob. The convex hull results are shown in Fig. 9(h) and Fig. 9(k). It can be seen that in convex hull draws the limits of the up, bottom, left and right edges of the lines. These edge points can be used as reference for the deviation of the line to determine evenness.

The next process is to draw a reference line from the top-most and bottom-most points of the convex hull. This is done by using a different color, to differentiate between the projected laser line (processed) and the reference line. The reference line is drawn in red color, while the processed lines are in white. The results are shown in Fig. 9(i) and Fig. 9(l).

After drawing the red line, it can be seen that the uneven wall from Fig. 9(l) has (white) lines deviating from the reference line. From Fig. 9(i) and Fig. 9(l), the deviation from the drawn red reference line can be calculated by using (1);

$$D_{wr} = \frac{\sum(P_{w_i} - P_{r_i})}{i_{wr}} \quad (1)$$

Where D_{wr} represents the indicator value for deflection between white and red dots, Pw represents the coordinates of the white dot, P_r represents the coordinates of the red dot and i_{wr} represents the number of white and red dots used in the process. If this indicator value is large, then it means that there are a lot of deflections of the white red with the red line. This can be used to classify that the wall is uneven. The distance between the camera and the wall set is 800mm. The resolution of the image captured is 1920 x 1080. The results of the tests for the uneven and even wall images are shown in Table II. The values are the average deviation of pixels from the reference line. The results obtained for six images, and three images are uneven walls.

TABLE II. AVERAGE PIXEL DEVIATION FOR EVEN AND UNEVEN WALL

Criteria	Image	Even Wall Image	Uneven Wall Image
Deviation (pixel)	1	13.39	53.18
	2	10.99	25.98
	3	11.36	30.57

Based on the results in Table II, the Even wall results shows that pixel deviation is lower than 15. The uneven wall has higher values of more than 20 for the images captured. The proposed method has shown that the deviation of the line is quantifiable and can be used to differentiate between even wall and uneven wall surface. At present, the deviations are measured for the vertical lines, but could be extended to horizontal lines in the future.

V. CONCLUSION

This research proposed a new method of assessing the wall surface evenness for quality assessment of internal building works. This approach uses vision-based method by capturing the images of the wall with the projected laser lines. The robot captures images of the wall in front while sliding to the left and pausing during capturing images to ensure the images are stable. The motion was implemented using four Mecanum wheels. Results show that the pixel deviation values can be used as an indicator to distinguish between even wall and uneven wall surface. The uniqueness of the proposed method is the use of fast image processing technique that does not use training data sets and the use of cost-effective devices such as laser-leveler and standard High Definition USB cameras available in the market instead of high cost sensors [10].

At present, the results shown are from concrete walls with a single color. Future work includes the testing of mixed wall colors and different wall surface types such as wood, foam or other types of materials. Other criteria should also be investigated, such as wall hollowness, cracks and damages.

ACKNOWLEDGMENT

Authors would like to acknowledge Construction Research Institute of Malaysia (CREAM) and Universiti Teknikal Malaysia Melaka for this collaborative research project.

REFERENCES

[1] J. S. Albus, “Trip Report: Japanese Progress in Robotics for Construction” Elsevier Science Publishers, B.V (North-Holland), 1986.

[2] D. Wallace, Y. H. He, J. Chagas Vaz, L. Georgescu and P. Y. Oh, "Multimodal Teleoperation of Heterogeneous Robots within a Construction Environment," 2020 IEEE/RSJ International Conference on Intelligent Robots and Systems (IROS), 2020, pp. 2698-2705, doi: 10.1109/IROS45743.2020.9340688.

[3] J. Sustarevas, K. X. Benjamin Tan, D. Gerber, R. Stuart-Smith and V. M. Pawar, "YouWasps: Towards Autonomous Multi-Robot Mobile Deposition for Construction," 2019 IEEE/RSJ International Conference on Intelligent Robots and Systems (IROS), 2019, pp. 2320-2327, doi: 10.1109/IROS40897.2019.8967766.

[4] E. Asadi, B. Li and I. Chen, "Pictobot: A Cooperative Painting Robot for Interior Finishing of Industrial Developments," in IEEE Robotics & Automation Magazine, vol. 25, no. 2, pp. 82-94, June 2018, doi: 10.1109/MRA.2018.2816972.

[5] N. Melenbrink, P. Michalatos, P. Kassabian and J. Werfel, "Using local force measurements to guide construction by distributed climbing robots," 2017 IEEE/RSJ International Conference on Intelligent Robots and Systems (IROS), 2017, pp. 4333-4340, doi: 10.1109/IROS.2017.8206298.

[6] C. Brosque, E. Galbally, O. Khatib and M. Fischer, "Human-Robot Collaboration in Construction: Opportunities and Challenges," 2020 International Congress on Human-Computer Interaction, Optimization and Robotic Applications (HORA), 2020, pp. 1-8, doi: 10.1109/HORA49412.2020.9152888.

[7] J. H. Lee, J. Park and B. Jang, "Design of Robot based Work Progress Monitoring System for the Building Construction Site," 2018 International Conference on Information and Communication Technology Convergence (ICTC), 2018, pp. 1420-1422, doi: 10.1109/ICTC.2018.8539444.

[8] M. A. V. J. Muthugala, M. Vega-Heredia, A. Vengadesh, G. Sriharsha and M. R. Elara, "Design of an Adhesion-Aware Façade Cleaning Robot," 2019 IEEE/RSJ International Conference on Intelligent Robots and Systems (IROS), 2019, pp. 1441-1447, doi: 10.1109/IROS40897.2019.8967978.

[9] M. Benndorf, T. Haenselmann, M. Garsch, N. Gebbeken, C.A. Mueller, T. Fromm, T. Luczynski, A. Birk, “Robotic Bridge Statics Assessment Within Strategic Flood Evacuation Planning using Low-Cost Sensors,” 2017 IEEE International Symposium on Safety, Security and Rescue Robotics (SSRR), Shanghai, China, 2017.

[10] R.J. Yan, E. Kayacan, I.M. Chen, K.T. Lee “QuicaBot: Quality Inspection and Assessment Robot,” IEEE Trans. on Automation Science and Engineering, vol. 16, no. 2, pp. 506-517, 2019.

[11] A. Sioma, “Automated Control of Surface Defects on Ceramic Tiles Using 3D Image Analysis”, MDPI Journals - Materials, Vol. 13, No. 1250, pp. 1-13, 2020.

[12] X. Li, L. Shen, Z. Ming, C. Zhang, H. Jiang, “Laser-based on-line machine vision detection for longitudinal rip of conveyor belt”, Optics, Elsevier, pp.360-369, 2018.

[13] H. Yang, Y. Jiang, F. Deng, Y. Mu, Y. Zhong, D. Jiao, “Detection of Bubble Defects on Tire Surface Based on Line Laser and Machine Vision”, MDPI Journals – Processes, Vol 10. No. 2, pp. 1-14, 2022.

[14] D.L. Escogido, A.D. Luca, “2-D High Precision Laser Sensor for Detecting Small Defects in PCBs”, 2012 9th International Conference on Electrical Engineering, Computing Science and Automatic Control (CCE), 2012.

[15] J.R.Araújo, A.G. Díaz, “Automated in-Line Defect Classification and Localization in Solar Cells for Laser-Based Repair”, -2014 IEEE 23rd International Symposium on Industrial Electronics (ISIE), 2014.

[16] D.G. Woo, J.K. Oh, C.H. Lee, S.H. Lee, S.H. Jung, “Development of a Multi-Line Laser Sensor Based Robotic 3D Measurement System”, 2011 11th International Conference on Control, Automation and Systems, pp. 1777-1782, 2011.

[17] T. Lei, H. Wang, P.Xiong, Y. Huang, H.Liu, “Laser Vision Detection Method for the Thermal Deformation of Tubesheet Welding”, 2019 4th International Conference on Robotics and Automation Engineering, pp. 116-119, 2019.

[18] Z. Liu , S.Wu, Q. Wu, C. Quan, and Y. Ren,” A Novel Stereo Vision Measurement System Using Both Line Scan Camera and Frame

Camera", IEEE Transactions on Instrumentation and Measurement, Vol. 68, No. 10, pp. 3563-3575, 2019.

[19] S. Pasinetti, G.Sansoni, F. Docchio, "In-line monitoring of laser welding using a smart vision system", 2018 Workshop on Metrology for Industry 4.0 and IoT, 2018, doi: 10.1109/METROI4.2018.8428332.

[20] W. Xiuping, B. Ruilin, L. Ziteng,"Weld Seam Detection and Feature Extraction Based on Laser Vision," Proceedings of the 33rd Chinese Control Conference, pp. 8249-8252, Nanjing, 2014, doi: 10.1109/ChiCC.2014.6896382.

[21] Yuanyuan Zo, Shang Cai, Pengfei Li, Kezhu Zuo, "Features Extraction of Butt Joint for Tailored Blank Laser Welding Based on Three-line Stripe Laser Vision Sensor," 2017 29th Chinese Control And Decision Conference (CCDC), pp.. 7736-7739, Chongqing, China, 2017, doi: 10.1109/CCDC.2017.7978594.